Supplementary Information (SI) for Nanoscale.

Electronic Supplementary Information for: Functionalisation of graphite and thermally reduced graphene oxide with bis-hydrazone copper(I) nitrate salt

Piotr W. Zabierowski,*[a] Lukáš Děkanovský,[a] Vlastimil Mazánek,[a] Maciej Hodorowicz[b] and Zdeněk Sofer*[a]

Contents

List of Tables

List of Figures

1 Materials and methods

The syntheses were carried out under inert atmosphere in ethanol (99.8%, Carlo Erba). Phthalaldehyde (99%) and 2-hydrazinopyridine (99%) were purchased from Flurochem, and used without further purification. Hydrazinopyridine is susceptible to moisture and after prolong contact with air turns to orange oil, affecting the synthesis outcome. Copper(II) nitrate trihydrate was purchased from Sigma Aldrich at a purity of 99%. Methanol (99.8%, Carlo Erba) was used as solvent for functionalisation. Triethlamine (99.9%) was also used as received from the manufacturer (Sigma Aldrich). Thermally reduced graphene oxide was obtained by Hummer's method [2] and further thermally reduced in presence of hydrazine (Elemental analysis found: N (%): 0.54; C (%): 85.81; H (%): 1.47; S (%): 0.36)) and graphite was milled (Elemental analysis found: N (%): 0.70; C (%): 97.41; H (%): 0.84; S (%):-).

1.1 Preparation of complex 1

Phthalaldehyde (66 mg, 0.50 mmol) and 2-hydrazinopyridine (109 mg, 1.00 mmol) were dispersed in 5 mL of ethanol (99.8%) under Ar atmosphere. The dispersion was heated at 75 °C for 10 min until full dissolution of the reagents. Thereafter, copper(II) nitrate trihydrate (120 mg, 0.496 mmol) was added and mixed until full dissolution. After few minutes of thermostating the reaction mixture at 75 °C the red crystalline product appeared. The mixture was decantated and precipitate was washed with 3 mL portion of ethanol (99.8%). The crystalline product (130 mg, 27.9%) was then dried in air at 75 °C. Elemental analysis calculated for $C_{38}H_{38}Cu_2N_{14}O_7$: C, 49.08%; H, 4.12%; N, 21.09%; S, -%. Found: C,48.1%; H,4.41%; N, 20.43%; S, -%. ^{1}H NMR (500 MHz, d_6-DMSO): δ 1.04-1.08 (7H, 1.06 (t, J = 6.99 Hz), 1.06 (t, J = 7.02 Hz)), 2.51 (22H, quint, J = 2.10 Hz), 3.33 (9H, s), 3.45 (4H, m), 7.05 (14H, m), 7.67 (4H, dd, J = 5.54, 3.47 Hz), 7.91 (5H, m), 7.98 (4H, s), 8.11 (5H, d, J = 6.75 Hz), 12.19 (1H, m), 12.17 (4H, s). ^{13}C NMR (126 MHz, d_6-DMSO): δ 56.50, 19.04, 109.28, 153.52, 146.58, 139.75, 138.97, 132.46, 129.19, 126.16, 117.53.HR-MS: m/z calcd for $C_{36}H_{32}Cu_2N_{12}$: 379.072694$[M]^{2+}$; 757.14649 $[M]^+$; found: 379.07312 $[M]^{2+}$; 757.13821 $[M]^+$. ATR FTIR (cm^{-1}): 3347br, 3213w, 2930br, 1617vs, 1540s, 1482vs, 1423vs, 1337s, 1281s, 1255vs, 1127s, 1073s, 1044m, 1006m, 763vs, 482m. UV-VIS: DMF, λ_{max} [nm] (ϵ, [$M^{-1}cm^{-1}$]) 298 (51175), 352 (50138)

1.2 Preparation of TRGO_Cu2 hybrid composite

TRGO (20.9 mg) and $[Cu_2L_2][NO_3]_2 \cdot C_2H_5OH$ (5.0 mg) were dispersed in 5 mL of methanol under Ar atmosphere, then 0.1 mL of triethylamine has been added and the dispersion was heated at 75 °C for one week. Then, the solid has been centrifuged at 30065 rcf for 15 min, washed with 1.5 mL of methanol and again centrifuged at 30065 rcf for 15 min. The supernatant has been discarded and the solid dried at 80 °C for 24h. Elemental analysis found: C,80.67%; H,1.69%; N, 2.75%; S, 0.31%.

1.3 Preparation of graphite_Cu2 hybrid composite

Graphite (20.9 mg) and $[Cu_2L_2][NO_3]_2 \cdot C_2H_5OH$ (5.5 mg) were dispersed in 5 mL of methanol under Ar atmosphere, then 0.1 mL of triethylamine has been added and the dispersion was heated at 75 °C for one week. Then, the solid has been centrifuged at 30065 rcf for 15 min, washed with 1.5 mL of methanol and again centrifuged at 30065 rcf for 15 min. The supernatant has been discarded and the solid dried at 80 °C for 24h. Elemental analysis found: C,94.86%; H,0.81%; N, 1.22%; S, -%.

1.4 Preparation of single crystals of complex 2

Phthalaldehyde (33 mg, 0.25 mmol) and 0.916 mL of isopropanolic solution of 2-hydrazinopyridine (68 mg/mL) were mixed and heated in a capped 8 mL vial at 75 °C until full dissolution of reagents. Thereafter, ammonium fluoride (56 mg, 1.5 mmol) was added together with copper(II) nitrate trihydrate (49 mg, 0.20 mmol) and 10 μL of pyridine. The red-brown solution was thermostated at 75 °C for two days. The block crystals were dark brown colored and occur in presence of crystals of complex 1. Therefore, the compound has been analysed only by SCXRD and FT-IR on single crystal selected from the batch.

1.5 Characterisation

Microanalyses on carbon, hydrogen, nitrogen and sulfur were performed using the Elementar vario EL Cube. The accuracy of the method is specified by the manufacturer for the simultaneous analysis of 5 mg of the standard 4-amino-benzene sulfonic acid in the module CHNS to 0.1% abs. for each element. The analysis results include all combustible sulfur, i.e. both organic and inorganic (S^{2-}, SO_4^{2-}), as well as all combustible carbon, i.e. both organic and inorganic (CO_3^{2-}).

1.5.1 X-ray crystal structure, data collection

Diffraction intensity data for single crystals of the new compounds were collected on a (supernova) KappaCCD (Nonius) diffractometer with graphite-monochromated MoKα radiation (λ = 0.71073 Å). Corrections for Lorentz, polarisation and absorption effects [Nonius, 1997-2000; [5]] were applied. The structure was solved by direct methods using SIR-92 program package[1] and refined using a full-matrix least square procedure on F^2 using SHELXL-97.[6] Anisotropic displacement parameters for all non-hydrogen atoms and isotropic temperature factors for hydrogen atoms were introduced. In the structure, the hydrogen atoms connected to carbon atoms were included in calculated positions from the geometry of molecules, whereas hydrogen atoms of water molecules were included from the difference maps and were refined with isotropic thermal parameters. The figures were made using Mercury.[3] CCDC-1590016 (for 1) and CCDC-2348643 (for 2) include the supplementary crystallographic data for this work. These data can be obtained free of charge from The Cambridge Crystallographic Data Centre via www.ccdc.cam.ac.uk/structures.

1.5.2 XPS

High-resolution XPS was performed with a SPECS spectrometer using an XR 50 MF monochromatic X-ray radiation source (1486.7 eV) and a Phoibos 150 2D CCD hemispherical analyzer and detector. The pressure inside the chamber during the experiments was set to 4×10^{-9} mbar or lower. Wide-scan surveys were obtained at Ep=100 eV, with subsequent high-resolution scans of the desired core lines carried out at Ep=20 eV with an acquisition step of 0.1 eV. The samples were placed on double-sided carbon tape. The binding energy values were referenced to the adventitious carbon peak at 284.8 eV. The Cu2p core level spectra were measured the first, to avoid copper/ligand oxidation in the X-ray beam.

1.5.3 Scanning electron microscopy (SEM)/ Energy-dispersive spectroscopy (EDS)

SEM coupled with EDS was employed to perform surface morphology characterization and elemental mapping analysis. Electron microscopy was conducted on Lyra 3 (Tescan).

1.5.4 Transmission Electron Microscopy

TEM with a JEOL 2200 FS microscope (Japan) was operated at an accelerating voltage of 200 kV. SAED patterns were obtained under the same conditions. Elemental analysis was conducted (Zeiss LIBRA 200 MC Cs scanning TEM, 200 kV) in high-angle annular dark-field scanning transmission electron microscopy mode, coupled with energy-dispersive X-ray analysis using a detector of Oxford instruments.

1.5.5 Raman spectra

Raman spectra were obtained using a Renishaw inVia confocal micro-Raman spectroscope (Renishaw) in backscattering geometry with a CCD detector, 532 nm DPSS laser, and 20x objective.

1.5.6 BET analysis

N_2 adsorption isotherms were measured at 77 K using a NOVAtouch series (Quantachrome Instruments, Anton Paar QuantaTec Inc., USA) to determine the BET area and characterize the pore size distribution of materials. The samples were first activated at 80 ^{o}C for 24 h, and N_2 was used as the adsorbate.

1.5.7 NMR spectroscopy

The NMR spectra were recorded on a 500 MHz instrument. The chemical shifts (δ) are indicated in ppm followed by integral intensity, multiplicity, corresponding coupling constants (J) in Hz. The ^{1}H and ^{13}C chemical shifts are referenced to a residual solvent signal (DMSO-d_6: 2.50 ppm for ^{1}H, 39.52 ppm for ^{13}C).

1.5.8 PXRD

XRD tests were carried out using a Bruker D8 Advance. The XRD patterns were obtained at 2-theta from 5^o to 50^o with a step of 0.02 degree and a integration time of 0.5 seconds.

1.5.9 DFT calculations

All the calculations presented in this article were performed with DFT methods using ORCA (version 5.0.0) software.[4] The B3LYP LANL2DZ level of theory was applied in all calculations.

1.5.10 ATR-FTIR spectroscopy

The IR spectra were recorded on a Thermo Scientific Nicolet iS5 FT-IR spectrometer equipped with an iD5 diamond ATR attachment. Advanced ATR correction was applied and the spectra were baseline corrected.

1.5.11 UV-VIS spectroscopy

The measurements of absorption spectra were performed at PerkinElmer LAMBDA 850+ UV/Vis Spectrophotometer (Shelton, CT, USA) in quartz cuvettes (10.00 mm optical path). The spectra were baseline corrected with the use of pure solvents: methanol, acetonitrile, N,N'-dimethylformamide and chloroform.

1.5.12 Electrochemical Impedance Spectroscopy

Impedance measurements were carried out at room temperature (in a vessel of 20 mL containing 2 mL of a given solvent) using an Autolab PGSTAT 204/FRA 32M potentiostat/galvanostat (Eco Chemie, Utrecht, The Netherlands) controlled by NOVA version 2.1 software (Eco Chemie). A sinusoidal potential modulation of 10 mV in amplitude in the 100 Hz to 100 kHz frequency range with a logarithmic scale of 10 points per decade was used. Interdigitated gold electrodes (5/5 μm, electrode/gap) produced by Micrux technologies

(Asturias, Spain) were used (ED-IDE3-Au) with the 2-electrode adapter matching the gas containing vessel. The interdigitated electrodes were washed in ethanol aided by sonication (30 min) and dried in a flow of Ar. Then the impedance spectra were collected for air atmosphere and in saturated atmospheres of different solvents. After the initial measurements, the surface of the interdigitated electrode was drop casted (3 μL) with suspensions of the hybrid composites (graphite-Cu2 and TRGO-Cu2) in dichloromethane (0.25 mg/mL), thereafter the electrodes were allowed to dry in air. The EIS of such electrodes were collected in vapours of different solvents.

1.6 Calculation of grain size from PXRD pattern for graphite_Cu2 hybrid composite

Given:

$\beta_{\text{FWHM}} = 0.29466$ degrees 2θ

$\lambda = 1.54$ Ångströms

$\theta = 27.21021$ degrees

The calculation will involve dividing the Bragg angle (θ) by 2 before converting it to radians. Then the Scherrer equation can be used:

Convert the Bragg angle (θ) from degrees to radians:

$$\theta_{\text{rad}} = \frac{\pi \cdot \theta}{180 \cdot 2}$$

$$\theta_{\text{rad}} = \frac{\pi \cdot 27.21021}{180 \cdot 2}$$

$$\theta_{\text{rad}} = 0.23725 \text{ radians}$$

The grain size can be calculated from the Scherrer equation:

$$D = \frac{K \cdot \lambda}{\beta_{\text{rad}} \cdot \cos(\theta_{\text{rad}})}$$

$$D = \frac{0.9 \cdot 1.54}{0.00513 \cdot \cos(0.23725)}$$

$$D = \frac{1.386}{0.00513 \cdot 0.972}$$

$$D = \frac{1.386}{0.004986}$$

$$D \approx 277.94 \text{ Å}$$

The calculated grain size using the Scherrer equation is approximately 277.94 Å.

For the graphite-Cu2 composite, given:

$$FWHM = 0.1834 \text{ deg}$$

$$\lambda = 1.54184 \text{ Å}$$

$$\theta = 26.96612 \text{ deg}$$

The Bragg angle θ must be converted from degrees to radians:

$$\theta_{\text{rad}} = \frac{\pi \times \theta}{180} = \frac{\pi \times 26.96612}{180} = 0.23518 \text{ rad}$$

The grain size can be calculated:

$$D = K \times \lambda / (FWHM_{\text{rad}} \times \cos(\theta_{\text{rad}}))$$

Substituting $K = 0.9$:

$$D = 0.9 \times 1.54184 / (0.1834 \times \cos(0.23518)) = 1.387656 / 0.003183 \times \cos(0.23518) \approx 448.63 \text{ Å}$$

Table S1: Crystallographic Data for Complex 1

Crystal data for Complex 1	
Chemical Formula	$C_{40}H_{44}Cu_2N_{14}O_8$
Mr	975.97
Crystal System, Space Group	Monoclinic, $P2_1/n$
Temperature (K)	130
a, b, c (Å)	15.4569 (4), 8.0238 (2), 17.5833 (5)
β (°)	92.358 (3)
V (Å^3)	2178.89 (10)
Z	2
Radiation Type	Mo Kα
μ (mm^{-1})	1.05
Crystal Size (mm)	0.20 × 0.10 × 0.10
Data collection	
Diffractometer	SuperNova, Dual, Cu at zero, Atlas
Absorption Correction	Multi-scan CrysAlis PRO 1.171.38.41r Empirical absorption correction using spherical harmonics, implemented in SCALE3 ABSPACK scaling algorithm.
Tmin, Tmax	0.831, 1.000
No. of measured, independent and observed [I > 2σ(I)] reflections	8691, 4961, 3282
Rint	0.041
(sin θ/λ)max (Å^{-1})	0.674
Refinement	
R[F^2 > 2σ(F^2)], wR(F^2), S	0.047, 0.101, 1.00
No. of reflections	4961
No. of parameters	301
H-atom treatment	H atoms treated by a mixture of independent and constrained refinement
$\Delta\rho$ max, $\Delta\rho$ min (e Å^{-3})	0.41, -0.39

Table S2: Crystallographic Data for Complex 2

Crystal data for Complex 2	
Chemical Formula	$C_{18}H_{16}CuN_8O_6$
Mr	503.93
Crystal System, Space Group	Orthorhombic, *Pbca*
Temperature (K)	130
a, b, c (Å)	17.9682 (3), 9.4647 (1), 23.1812 (5)
V (Å^3)	3942.28 (12)
Z	8
Radiation Type	Mo Kα
μ (mm^{-1})	1.17
Crystal Size (mm)	0.25 × 0.20 × 0.10
Data collection	
Diffractometer	XtaLAB Synergy, Dualflex, HyPix
Absorption Correction	Multi-scan CrysAlis PRO 1.171.38.41r Empirical absorption correction using spherical harmonics, implemented in SCALE3 ABSPACK scaling algorithm.
Tmin, Tmax	0.782, 1.000
No. of measured, independent and observed [I > 2σ(I)] reflections	17137, 4598, 3738
Rint	0.033
(sin θ/λ)max (Å^{-1})	0.674
Refinement	
R[F^2 > 2σ(F^2)], wR(F^2), S	0.040, 0.093, 1.08
No. of reflections	4598
No. of parameters	337
H-atom treatment	H atoms treated by a mixture of independent and constrained refinement
$\Delta\rho$ max, $\Delta\rho$ min (e Å^{-3})	0.49, -0.80

Table S3: Hydrogen-bond geometry for complex 1 (Å, °)

D—H···A	D—H	H···A	D···A	D—H···A
N2—H2A···O4^{i}	0.75(3)	2.05(3)	2.790(3)	170(3)
N5—H5A···O1^{ii}	0.85(3)	1.98(3)	2.827(4)	174(3)
C6—H6···O3^{i}	0.95	2.31	3.224(4)	160.7
C13—H13···O3^{iii}	0.95	2.47	3.343(4)	152.9
C17—H17···O2^{iv}	0.95	2.61	3.518(4)	159.0
C18—H18···O4	0.95	2.34	3.205(4)	151.0
O1—H21···O2^{v}	0.75(3)	2.31(3)	2.988(4)	150(3)
O1—H21···O3^{v}	0.75(3)	2.26(3)	2.956(4)	153(4)
O1—H21···N7^{v}	0.75(3)	2.65(3)	3.396(4)	172(3)

Symmetry codes: (i) $x+1/2$, $y1/2$, $z+1/2$; (ii) $x1$, y, z; (iii) $x1/2$, $y+1/2$, $z1/2$; (iv) x, $y+1$, $z+1$; (v) $x+1/2$, $y+1/2$, $z1/2$.

Table S4: Hydrogen-bond geometry for complex 2 (Å, °)

D—H···A	D—H	H···A	D···A	D—H···A
N2—H2A···O5^{i}	0.81(3)	2.01(3)	2.783(3)	158(3)
N5—H5A···O6^{ii}	0.80(3)	2.04(3)	2.800(3)	160(3)
C1—H1···O1A^{i}	0.95	2.57	3.260(9)	130.1
C1—H1···O1B^{i}	0.95	2.52	3.226(17)	131.0
C6—H6···O3B^{iii}	0.95	2.40	2.960(8)	117.4
C6—H6···O5^{i}	0.95	2.61	3.340(3)	134.2
C13—H13···O6^{iv}	0.95	2.55	3.188(3)	124.6
C17—H17···O5^{v}	0.95	2.49	3.345(3)	149.2

Symmetry codes: (i) x, $y+1/2$, $z+1/2$; (ii) $x+1/2$, $y+1$, $z+1/2$; (iii) x, $y1/2$, $z+1/2$; (iv) x, $y+1/2$, $z+1/2$; (v) x, $y+3/2$, $z+1/2$.

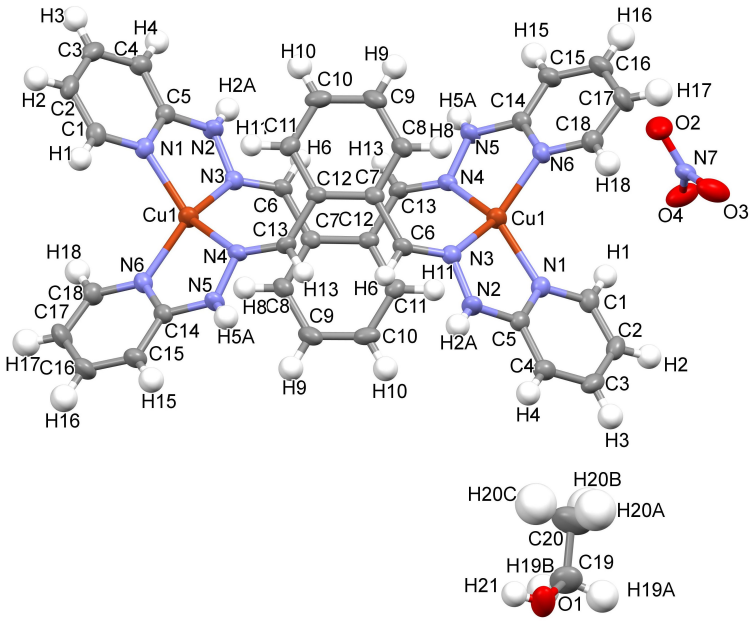

Figure S1: Molecular structure of Complex 1 with atom labelling. The thermal displacement ellipsoids are drawn with 50% probability. Selected bond distances (Å): Cu1-N1 2.023(2); Cu1-N3 2.029(2); N2-N3 1.374(3); N5-N4 1.379(3); C1-N1 1.357(3); O2-N7 1.271(4); O1-C19 1.426(5); N3-C6 1.294(3); C6-C7 1.452(4). Selected angles (°): N1-Cu1-N3 81.64(9); N2-N3-C6 114.8(2); N3-N2-C5 119.5(2); N2-C5-N1 116.7(2); N3-C6-C7 122.8(2).

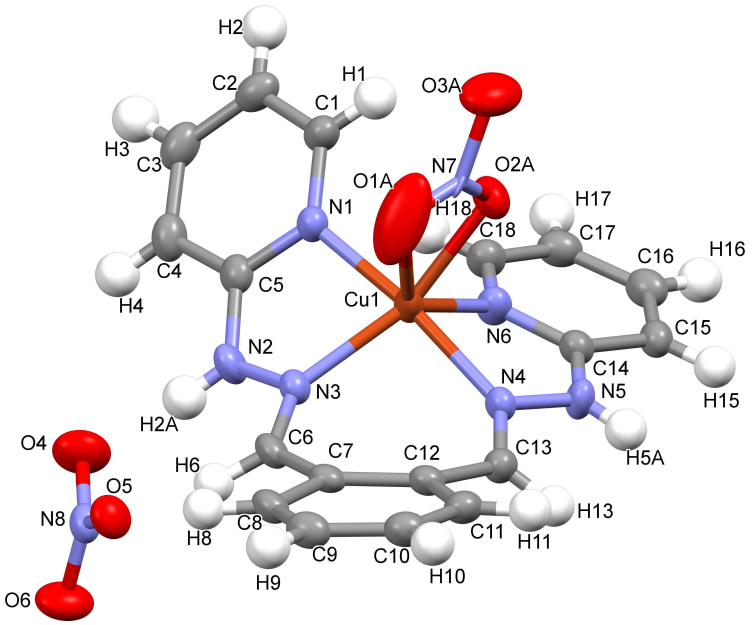

Figure S2: Molecular structure of Complex 2 with atom labelling. The thermal displacement ellipsoids are drawn with 50% probability. One set of atoms representing nitrate ion coordinated to copper has been omitted for clarity. Selected bond distances (Å):Cu1-O1A 2.55(1); Cu1-O2A 2.009(3); N1-Cu1 1.955(2); N3-Cu1 2.006(2); N4-Cu1 1.980(2); N6-Cu1 2.088(2); N2-N3 1.378(3); N1-C1 1.354(3); N4-N5 1.373(3); N5-C14 1.369(3); C14-N6 1.336(3); N7-O3A 1.36(1); C6-N3 1.279(3); C13-N4 1.281(3). Selected angles (°): N1-Cu1-N3 80.87(8); Cu1-N3-N2 106.7(1); N2-C5-N1 115.7(2); N3-Cu1-N4 94.50(8); N4-Cu1-N6 80.27(8); N1-Cu1-O2A 94.9(1); N6-Cu1-O1A 137.7(2); N4-Cu1-O2A 94.3(1); O1A-Cu1-O2A 52.5(3).

Table S5: Bond lengths in the structure of complex 1 (Å)

Atom1	Atom2	Length (Å)
Cu1	N1	2.023(2)
Cu1	N3	2.029(2)
Cu1	N4	2.068(2)
Cu1	N6	1.995(2)
N2	N3	1.374(3)
N4	N5	1.379(3)
N1	C1	1.357(3)
N1	C5	1.335(4)
N6	C14	1.339(4)
N6	C18	1.352(4)
C5	N2	1.370(3)
C14	N5	1.375(4)
N3	C6	1.294(3)
N4	C13	1.288(3)
C6	C7	1.452(4)
C13	C12	1.464(4)
C7	C8	1.393(4)
C11	C12	1.395(4)

Table S6: Angles in the structure of complex 1 (°)

Atom1	Atom2	Atom3	Angle (°)
N1	Cu1	N3	81.64(9)
N3	Cu1	N4	110.76(9)
N4	Cu1	N6	81.64(9)
N1	Cu1	N4	137.30(9)
N3	Cu1	N6	143.1(1)
N1	Cu1	N6	113.4(1)
N1	C5	N2	116.7(2)
C1	N1	C5	117.1(2)
N2	N3	C6	114.8(2)
N6	C14	N5	116.8(2)
C14	N5	N4	118.8(2)
N5	N4	C13	115.2(2)
C5	N2	N3	119.5(2)
Cu1	N6	C14	113.3(2)
C14	N6	C18	117.2(2)
N3	C6	C7	122.8(2)
C12	C13	N4	122.7(2)

Table S7: Bond lengths in the structure of complex 2 (Å)

Atom1	Atom2	Length (Å)
Cu1	O2A	2.009(3)
Cu1	O1A	2.55(1)
Cu1	N4	1.980(2)
Cu1	N6	2.088(2)
Cu1	N3	2.006(2)
Cu1	N1	1.955(2)
N2	N3	1.378(3)
N2	C5	1.370(3)
C5	N1	1.344(3)
N1	C1	1.354(3)
N4	N5	1.373(3)
N5	C14	1.369(3)
C14	N6	1.336(3)
C6	C7	1.466(3)
C13	C12	1.468(3)
N7	O1A	1.09(2)
N7	O2A	1.24(1)
N7	O3A	1.36(1)
N8	O4	1.240(3)
N8	O5	1.256(3)
N8	O6	1.237(3)

Table S8: Angles in the structure of complex 2 (°)

Atom1	Atom2	Atom3	Angle (°)
N1	Cu1	N3	80.87(8)
N1	Cu1	O1A	93.4(2)
N3	Cu1	N4	94.50(8)
N3	Cu1	O1A	96.8(2)
N4	Cu1	O2A	94.3(1)
N4	Cu1	N6	80.27(8)
N6	Cu1	O2A	85.3(1)
N6	Cu1	N1	93.93(8)
C14	N5	N4	118.9(2)
C12	C13	N4	127.3(2)
C7	C6	N3	125.6(2)
N3	N2	C5	116.3(2)
C5	N1	C1	119.1(2)
C13	N4	N5	117.2(2)
C14	N6	Cu1	109.7(2)
C12	C7	C8	118.4(2)
C14	N6	C18	118.0(2)
O2A	N7	O1A	126(1)
O1A	N7	O3A	123(1)
O4	N8	O5	120.7(2)
O5	N8	O6	119.8(2)

Table S9: Vibrational Frequencies, Absorption Coefficients, and Assignments for complex 1 at the B3LYP LANL2DZ level of theory in the gas phase

Wavenumber [cm^{-1}]	**Absorption Coefficient [a.u.]**	**Assignment**
482	0.010223	N-H scissoring with imine C-H
498	0.042713	Bending of -NH hydrazone groups
800	0.012938	C-H bending of the phenyl rings
806	0.052513	Bending of C-H in pyridine rings
806	0.019909	Out-of-plane C-H bending of pyridine rings
929	0.011158	C-H wagging of the imine
1092	0.071894	N-N stretching of the hydrazone group, wagging of the phenyl ring
1113	0.022752	N-N stretching of the hydrazone group, wagging of the phenyl ring
1137	0.013644	N-N stretching of the hydrazone group, wagging of the phenyl ring
1148	0.010851	C=C stretching together with hydrazone N-N stretching and wagging of pyridine protons
1151	0.040802	Rocking of C-H groups in pyridine and phenyl
1302	0.072029	N-C stretching of C-NH-N=

Continued on next page

Table S9 – Continued from previous page

Wavenumber [cm^{-1}]	**Absorption Coefficient [a.u.]**	**Assignment**
1302	0.017605	C=C stretching of pyridine rings, together with N-H wagging and N-N stretching
1360	0.031585	Imine C-H bending and pyridine ring C-C stretching/breathing
1369	0.009207	pyridine and phenylene breathing vibration
1456	0.013949	Wagging of C-H groups in pyridine rings
1508	0.109673	Rocking of pyridine rings
1509	0.040649	Wagging of C-H groups in pyridine rings
1556	0.096673	Bending of -NH-N and wagging of pyridine combination band
1561	0.028974	Imine -C-H and -N-H bending (waving/rocking) together with pyridine C-H bending
1593	0.010247	C=N tretching of the imine together with phenyl breathing
1603	0.028915	Hydrazone C=N stretching
1616	0.026357	Pyridine C=N stretching
1623	0.008295	C=N imine stretching together with C=N and C=C pyridine stretching
1647	0.143607	Wagging combination vibration of pyridine rings and phenyl ring
1648	0.067979	Rocking/breathing of pyridine rings
3109	0.020228	C-H stretching of the imine groups
3578	0.012019	Hydrazone N-H stretching

Table S10: Vibrational Frequencies, Absorption Coefficients, and Assignments for complex 2 at the B3LYP LANL2DZ level of theory in the gas phase

Wavenumber [cm^{-1}]	**Absorption Coefficient [a.u.]**	**Assignment**
457	0.01709	N-H bending
481	0.011036	Out-of-plane pyridine ring C-H wagging vibration together with phenyl wagging
806	0.025472	Out-of-plane pyridine ring C-H wagging vibration together with phenyl breathing
810	0.017725	O-Cu-O scissoring, pyridine and phenyl ring breathing
926	0.014865	N-N stretching, N-O stretching and pyridine C-H wagging in plane
1130	0.013434	N-O stretching together with hydrazone N-N stretching and pyridine and phenyl wagging of C-H
1158	0.057627	Pyridine C-C together with -NH- wagging

Continued on next page

Table S10 – Continued from previous page

Wavenumber [cm^{-1}]	**Absorption Coefficient [a.u.]**	**Assignment**
1307	0.034943	In-plane wagging of the -N(H)-N=C(H)- bonds, together with pyridine C-H wagging in plane and N-O stretching
1439	0.013487	N=O nitrate stretching together with wagging of pyridine C-H and hydrazone -C(H)=N-NH
1443	0.062984	Wagging of pyridine and imine -C-H, C=C stretching of pyridine
1472	0.028015	In-plane pyridine C-H wagging and C=N stretching of pyridine ring
1508	0.018575	C-N hydrazone stretching together with pyridine breathing
1510	0.03215	N-N stretching, NH-N-CH scissoring and C=C pyridine stretching
1551	0.016662	Pyridine breathing, -CH=N-NH- scissoring
1565	0.031671	C=N stretching in hydrazone groups
1644	0.01181	Imine C=N stretching together with pyridine breathing
1648	0.040567	Imine C=N stretching together with pyridine breathing
1654	0.053077	imine C=N stretching in hydrazone and in pyridine ring
3105	0.007283	imine -C-H stretching
3586	0.007181	Hydrazone -N-H stretching

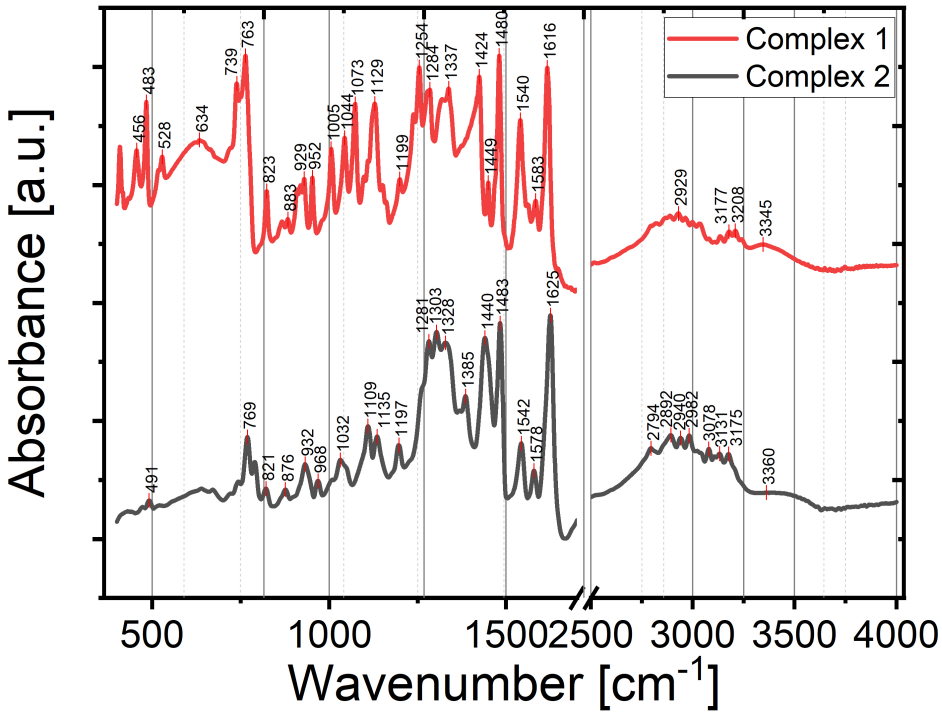

Figure S3: The ATR-FTIR spectra for crystals of complex 1 and 2 at room temperature.

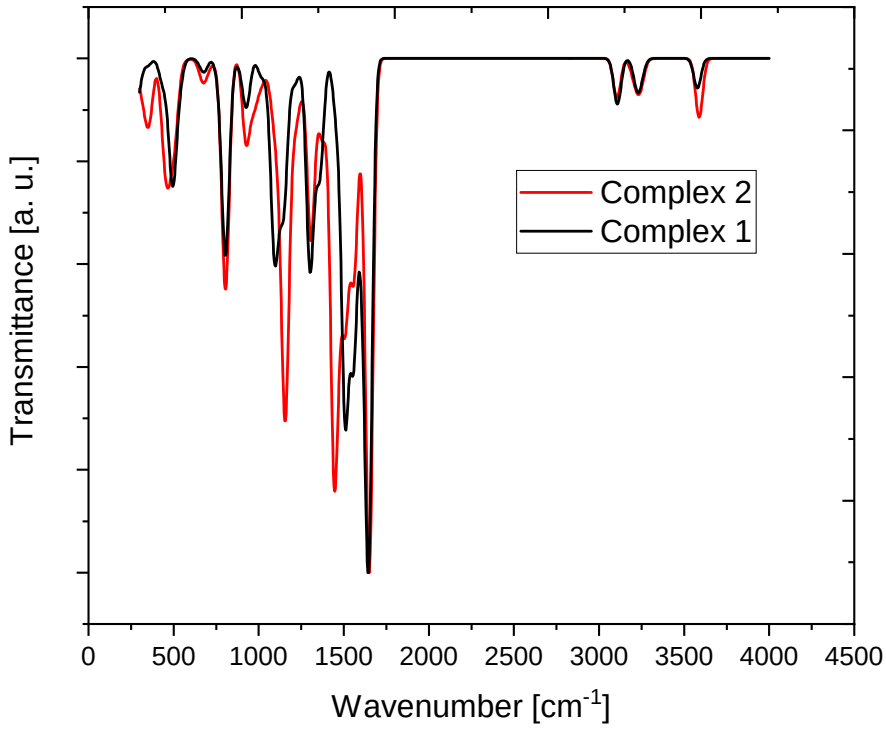

Figure S4: The simulated IR spectra at B3LYP LANL2DZ level of theory for $[Cu_2L_2]^2+$ (Complex 1) and $[CuL(NO_3)]^+$ (Complex 2).

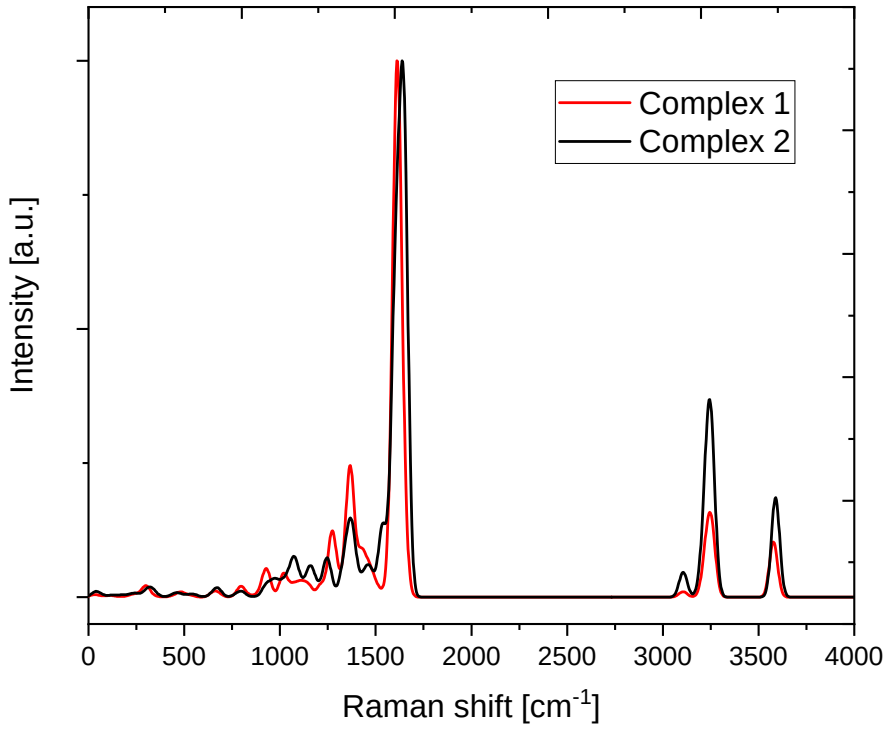

Figure S5: The simulated Raman spectra at B3LYP LANL2DZ level of theory for $[Cu_2L_2]^2+$ (Complex 1) and $[CuL(NO_3)]^+$ (Complex 2).

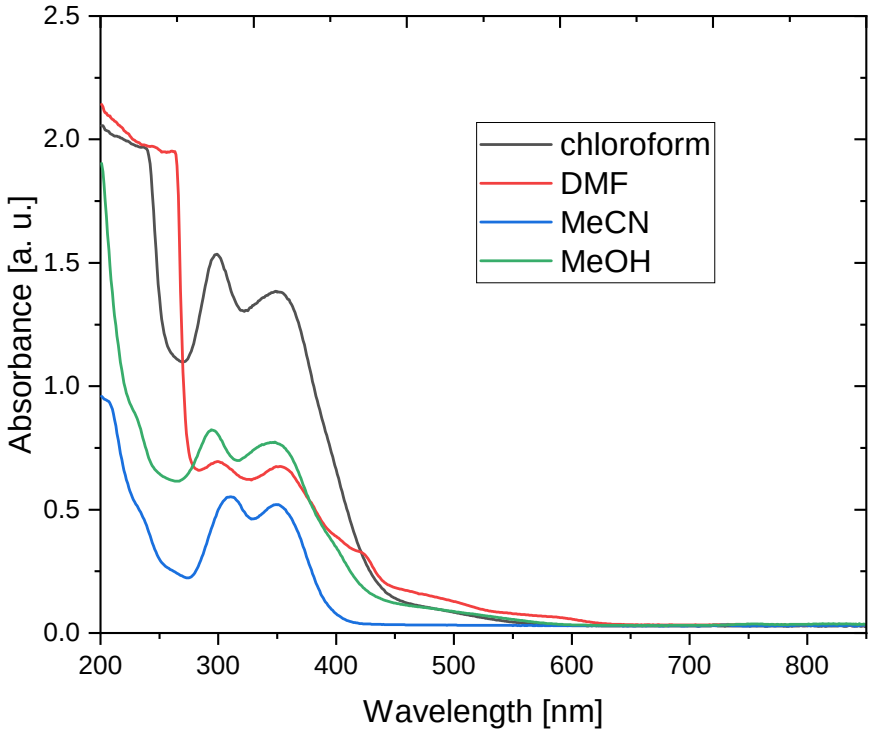

Figure S6: The absorption spectra of complex 1 in different solvents at room temperature.

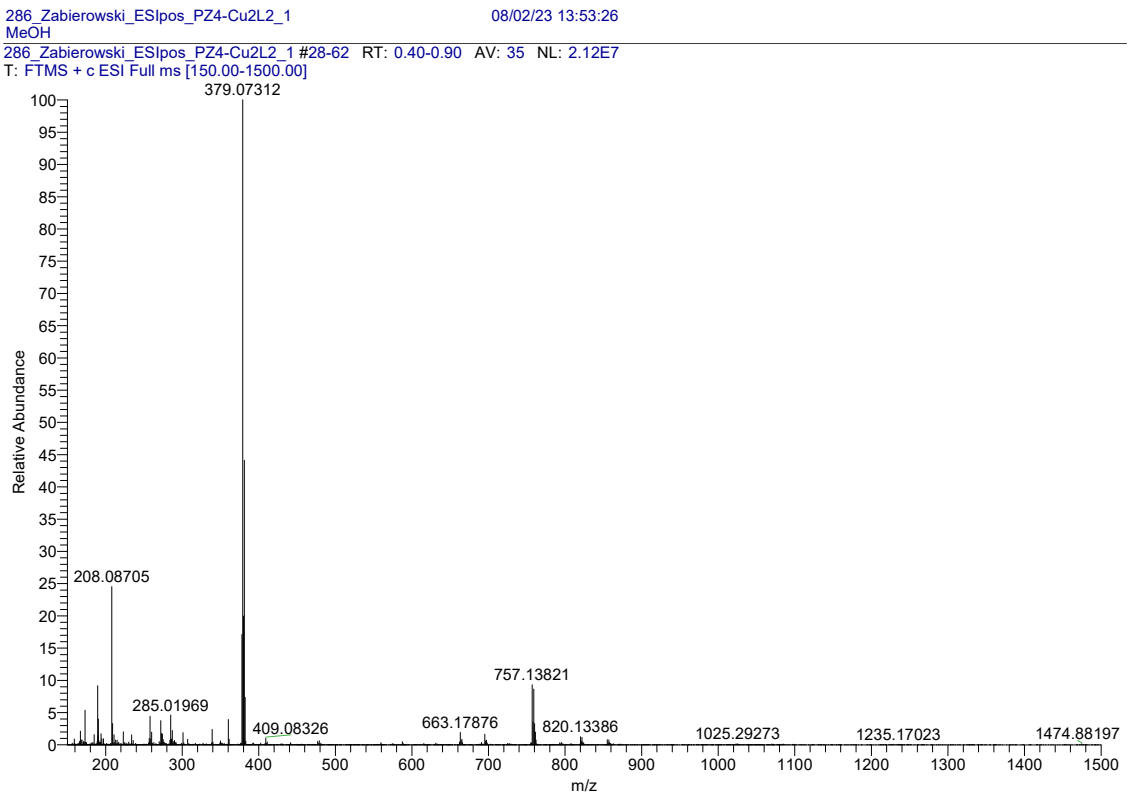

Figure S7: The HRMS spectrum for Complex 1 in methanol, positive mode of ionisation.

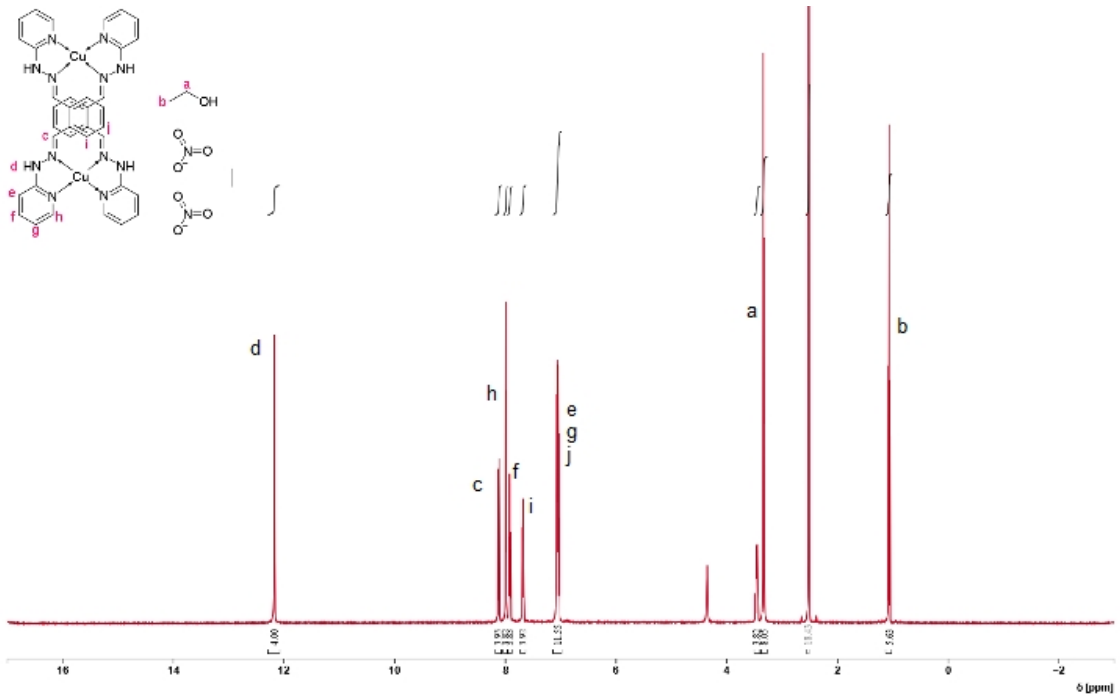

Figure S8: The ^{1}HNMR spectrum of complex 1 in d_6-DMSO at room temperature.

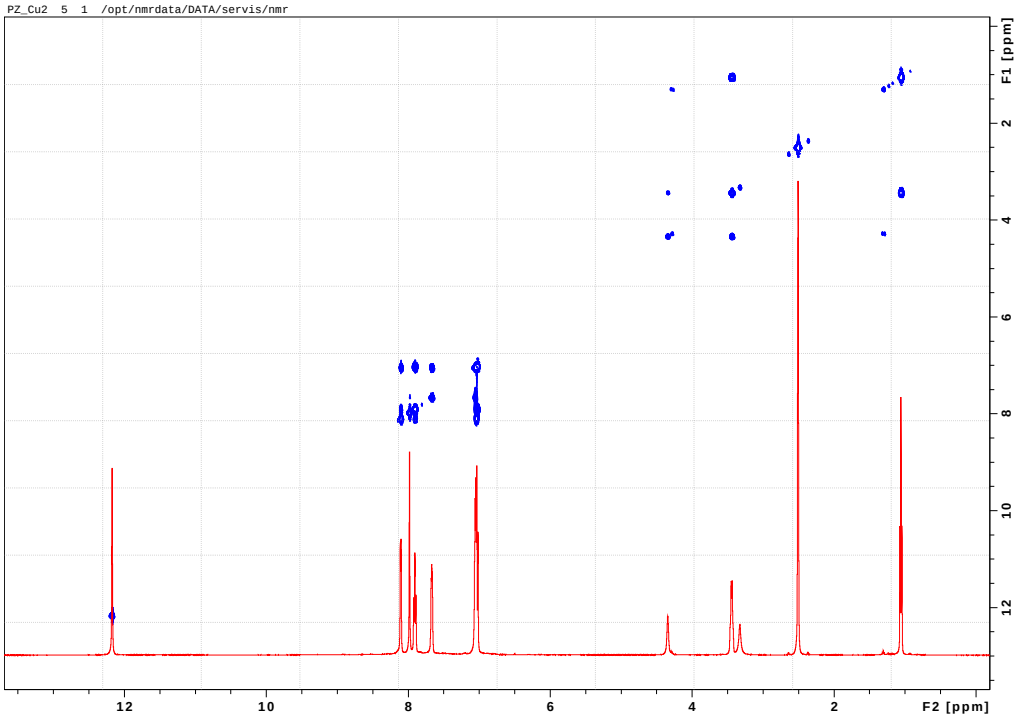

Figure S9: The COSY spectrum for complex 1 in d_6-DMSO at room temperature.

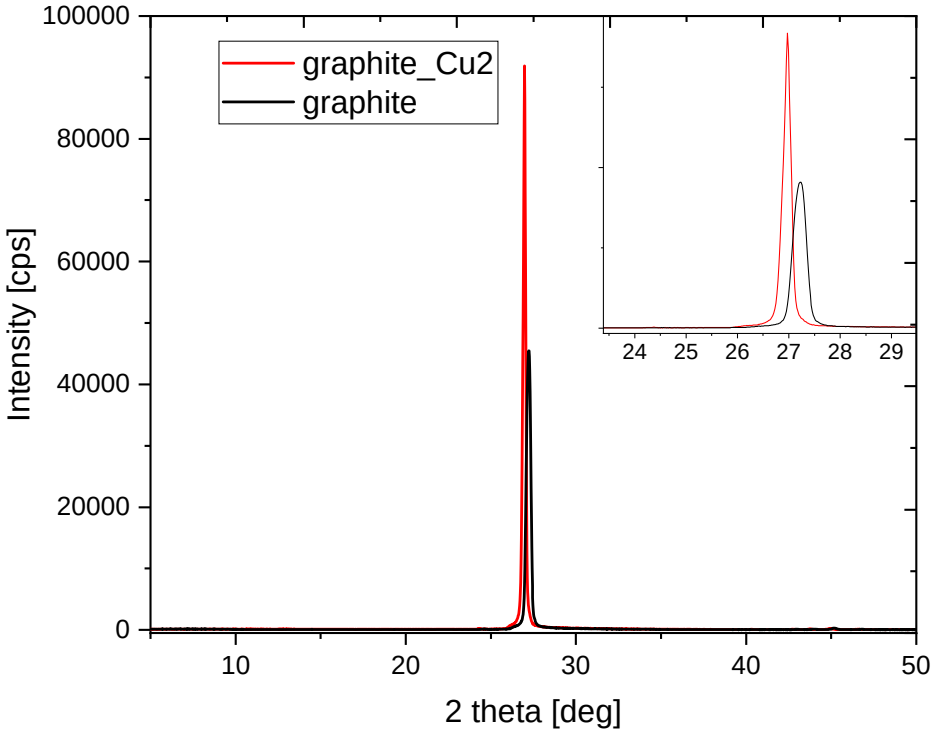

Figure S10: The powder diffractograms of graphite and graphite-Cu2 composite.

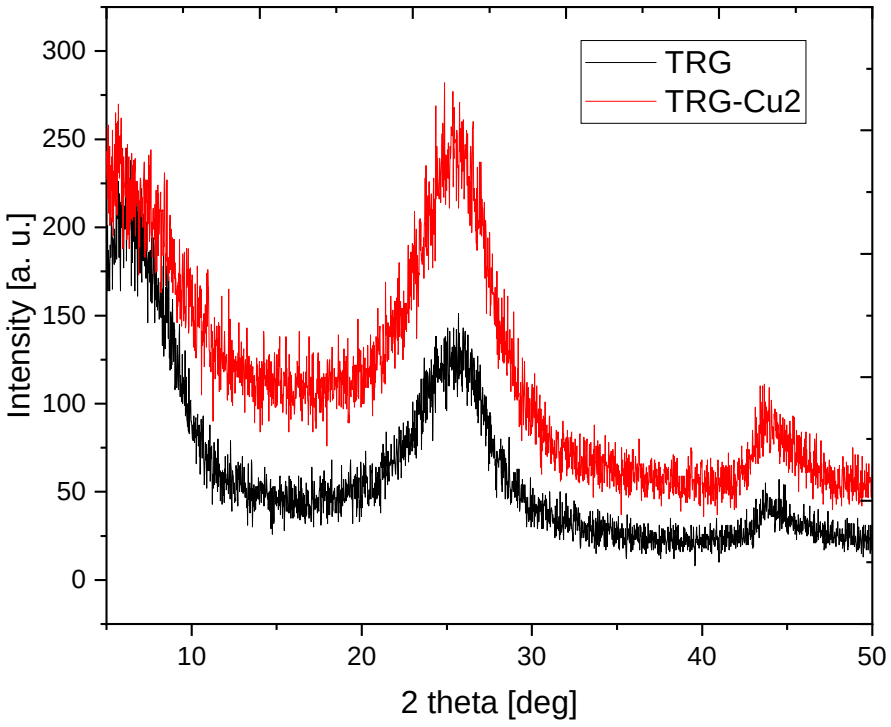

Figure S11: The powder diffractograms of TRGO and TRGO-Cu2 composite.

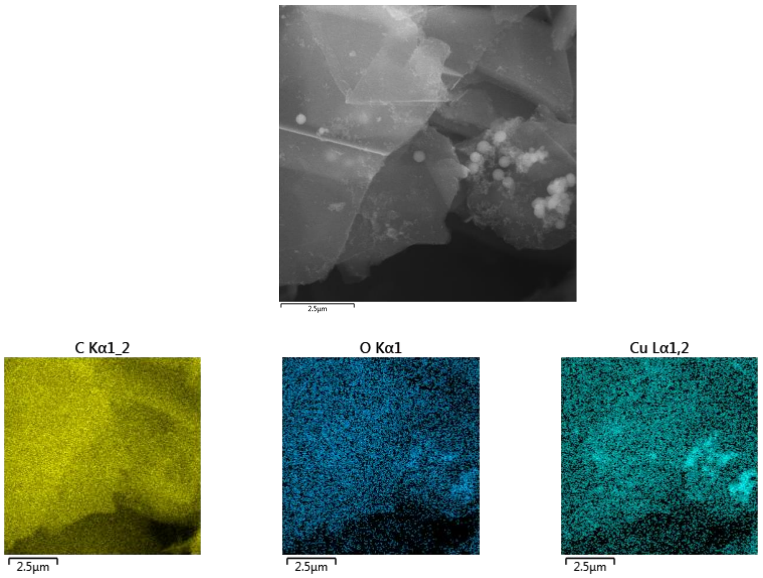

Figure S12: The FESEM images with elemental mapping for sample graphite-Cu2.

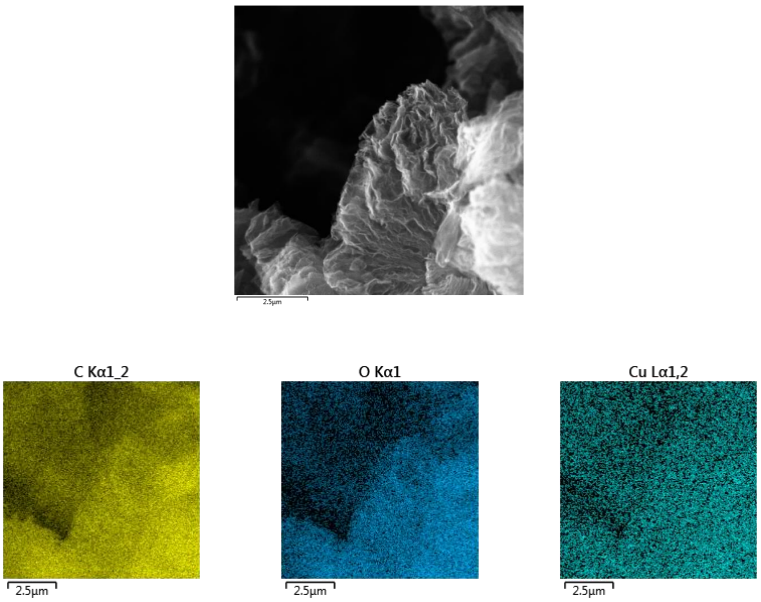

Figure S13: The FESEM images with elemental mapping for sample TRGO-Cu2.

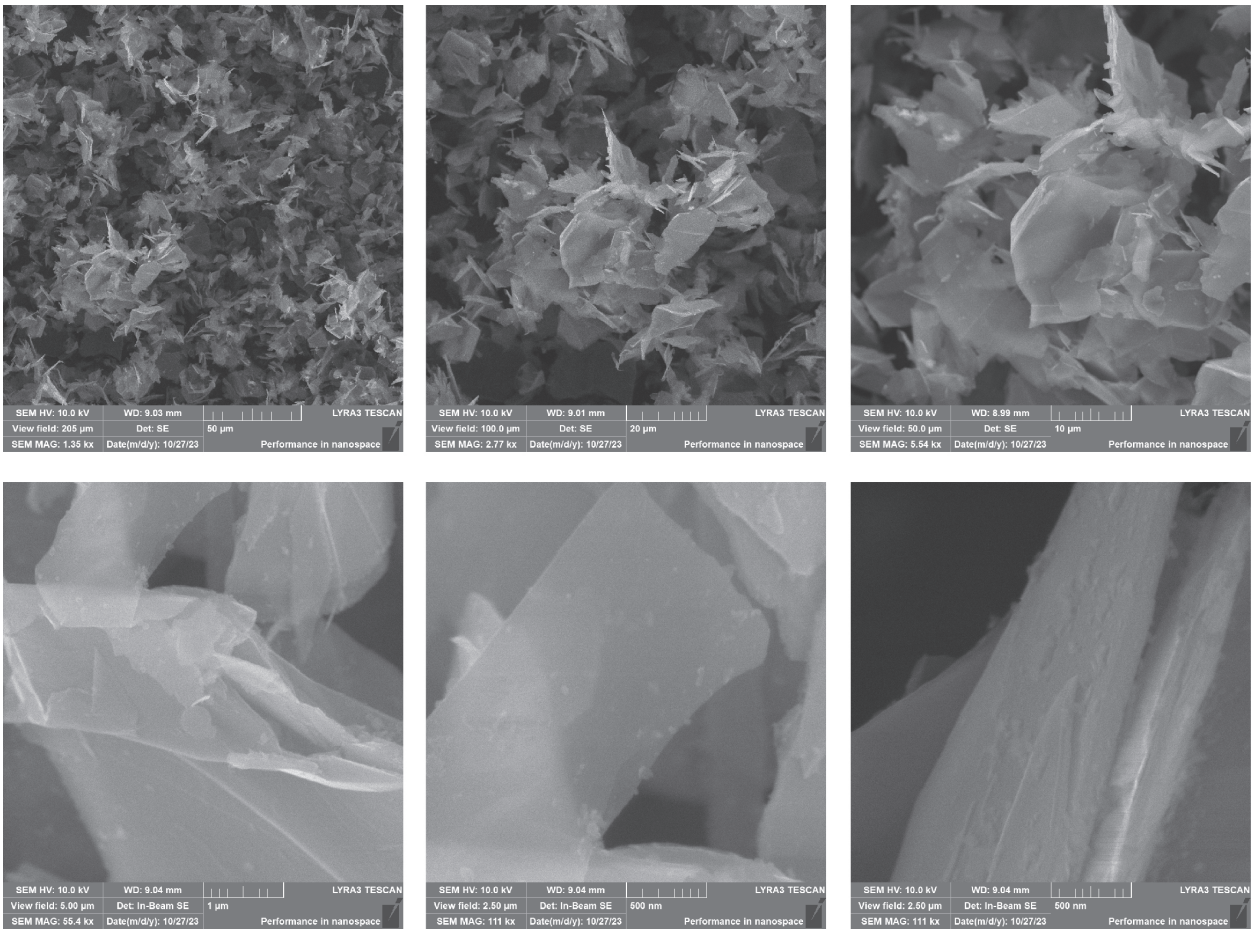

Figure S14: The FE-SEM images of graphite-Cu2 composite.

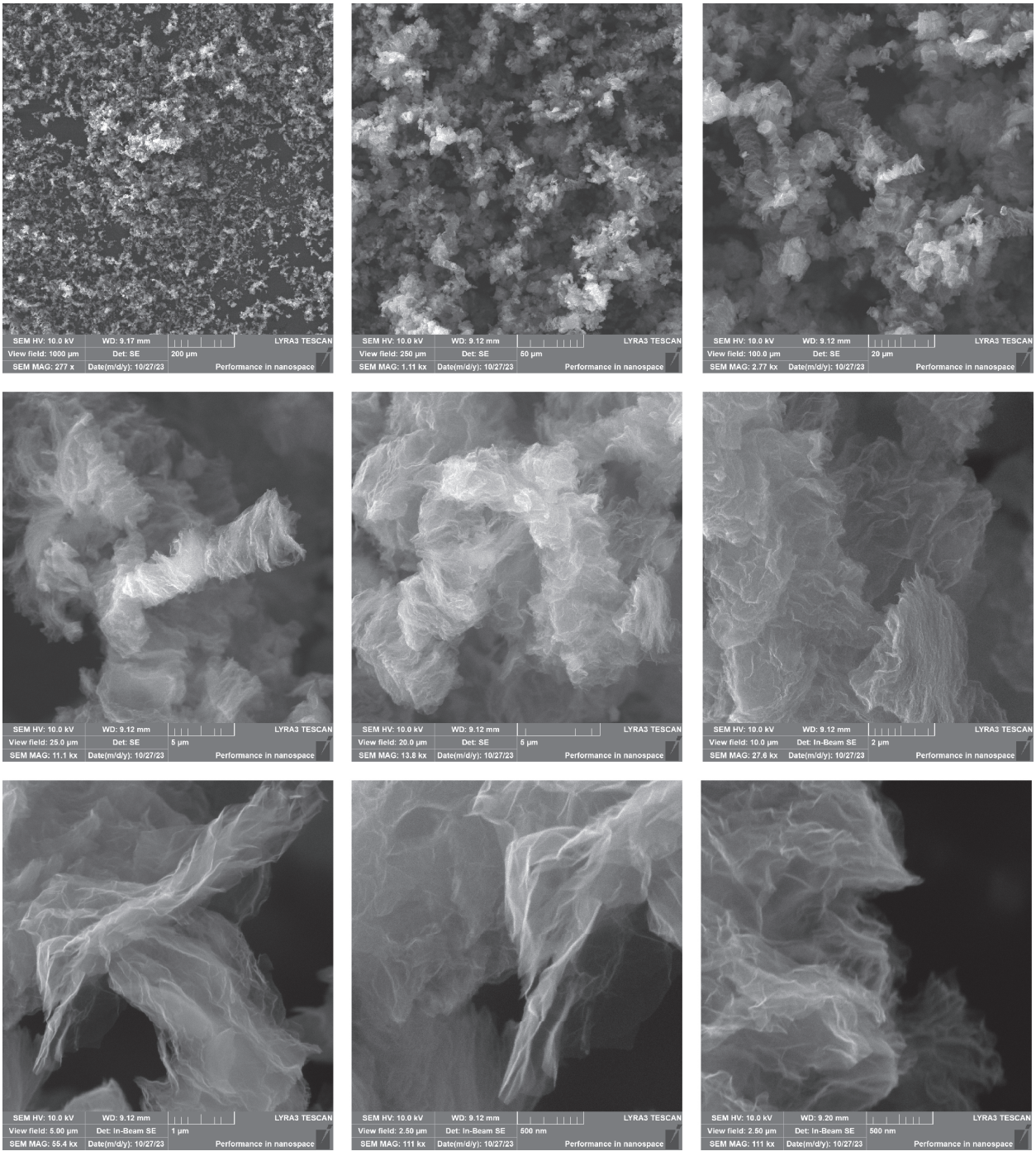

Figure S15: The FE-SEM images of TRGO-Cu2 composite.

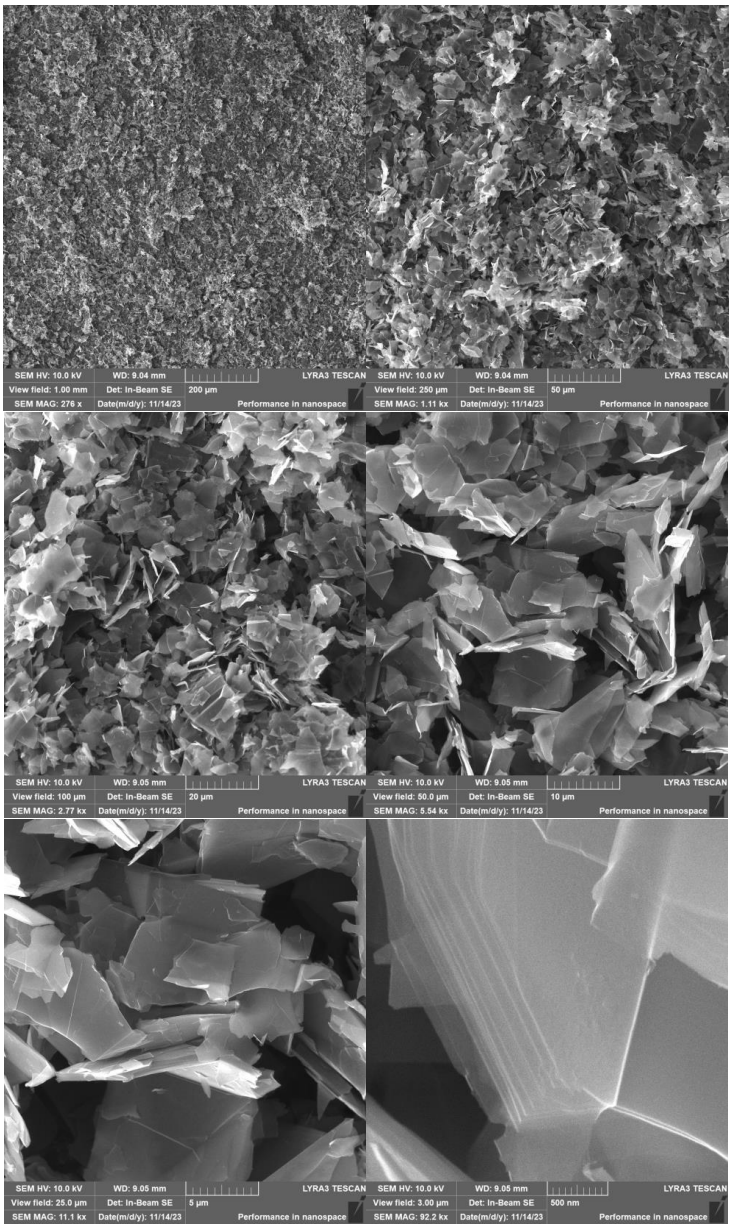

Figure S16: The FE-SEM images of graphite used in functionalisation.

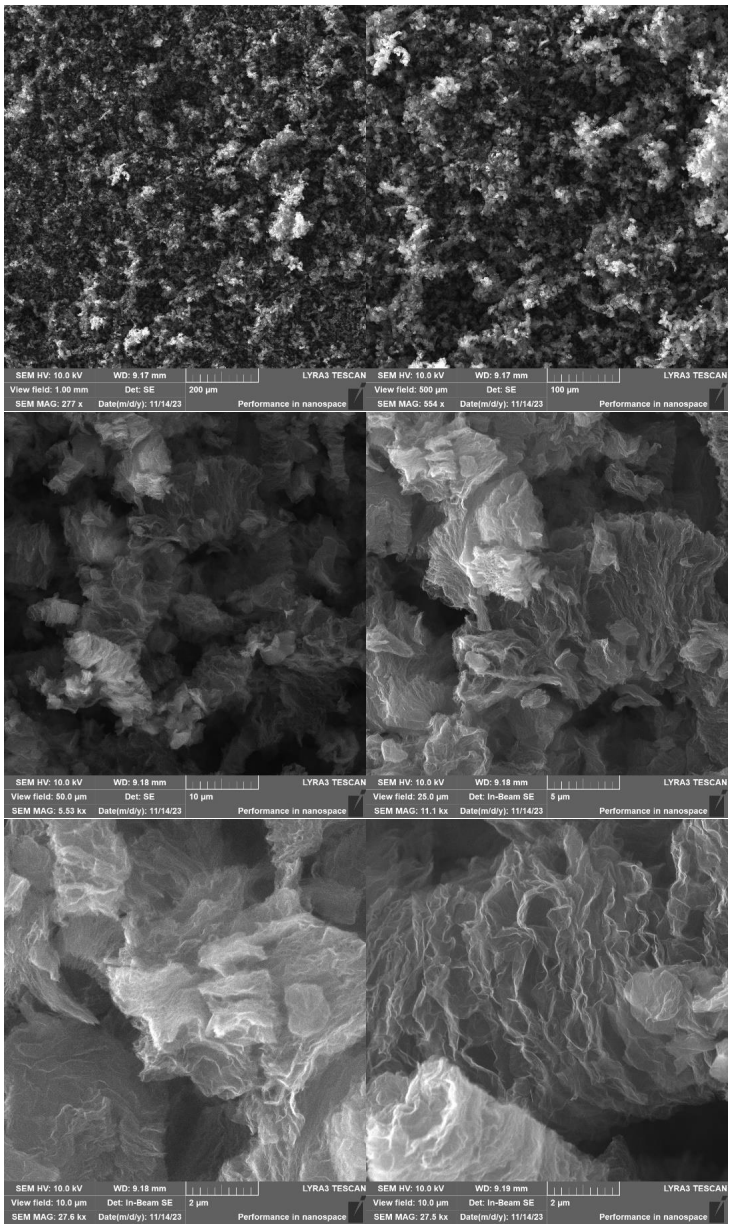

Figure S17: The FE-SEM images of TRGO used in functionalisation.

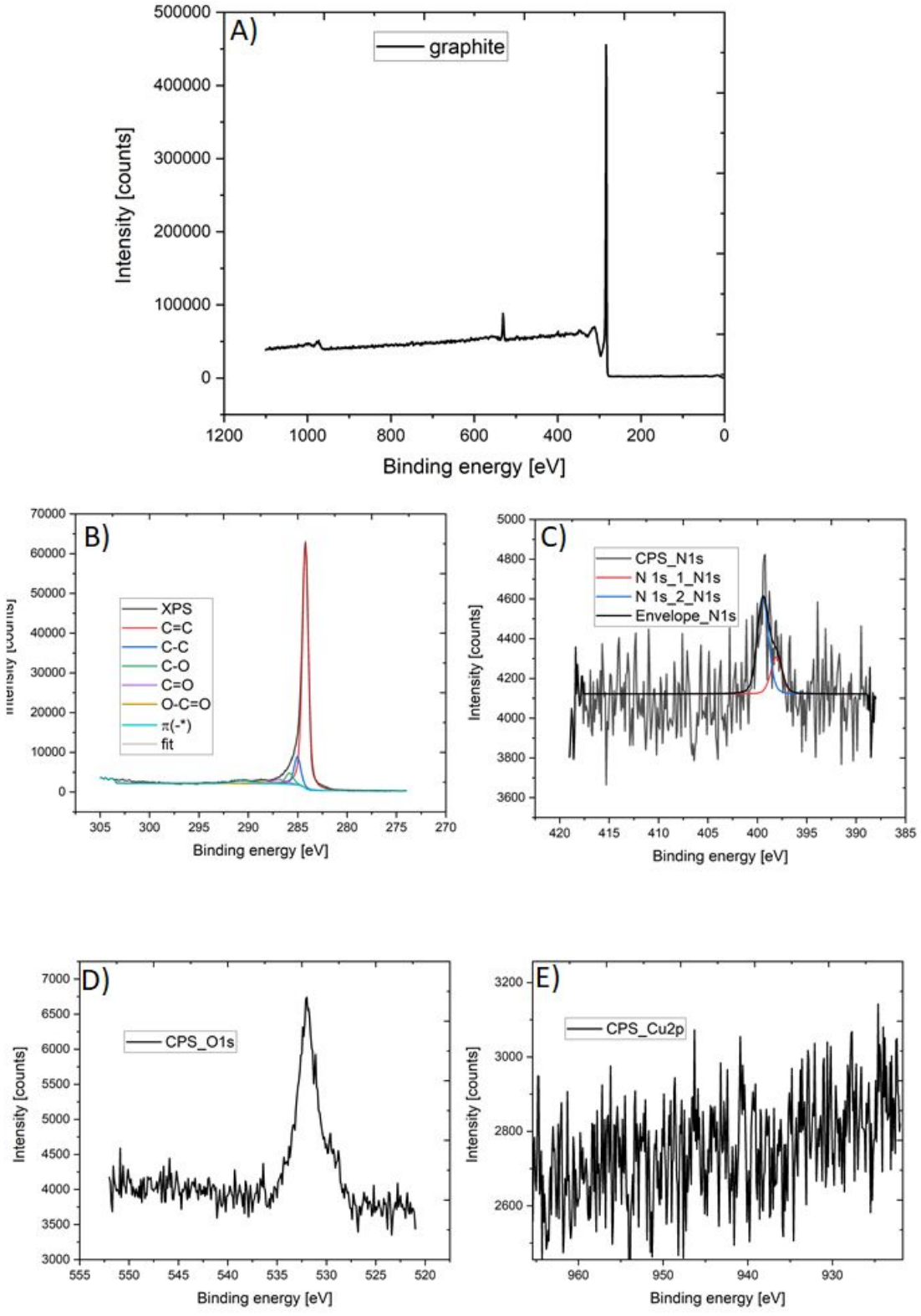

Figure S18: The XPS spectra for graphite: A) survey; B) C1s; C) N1s; D) O1s; E) Cu2p core levels.

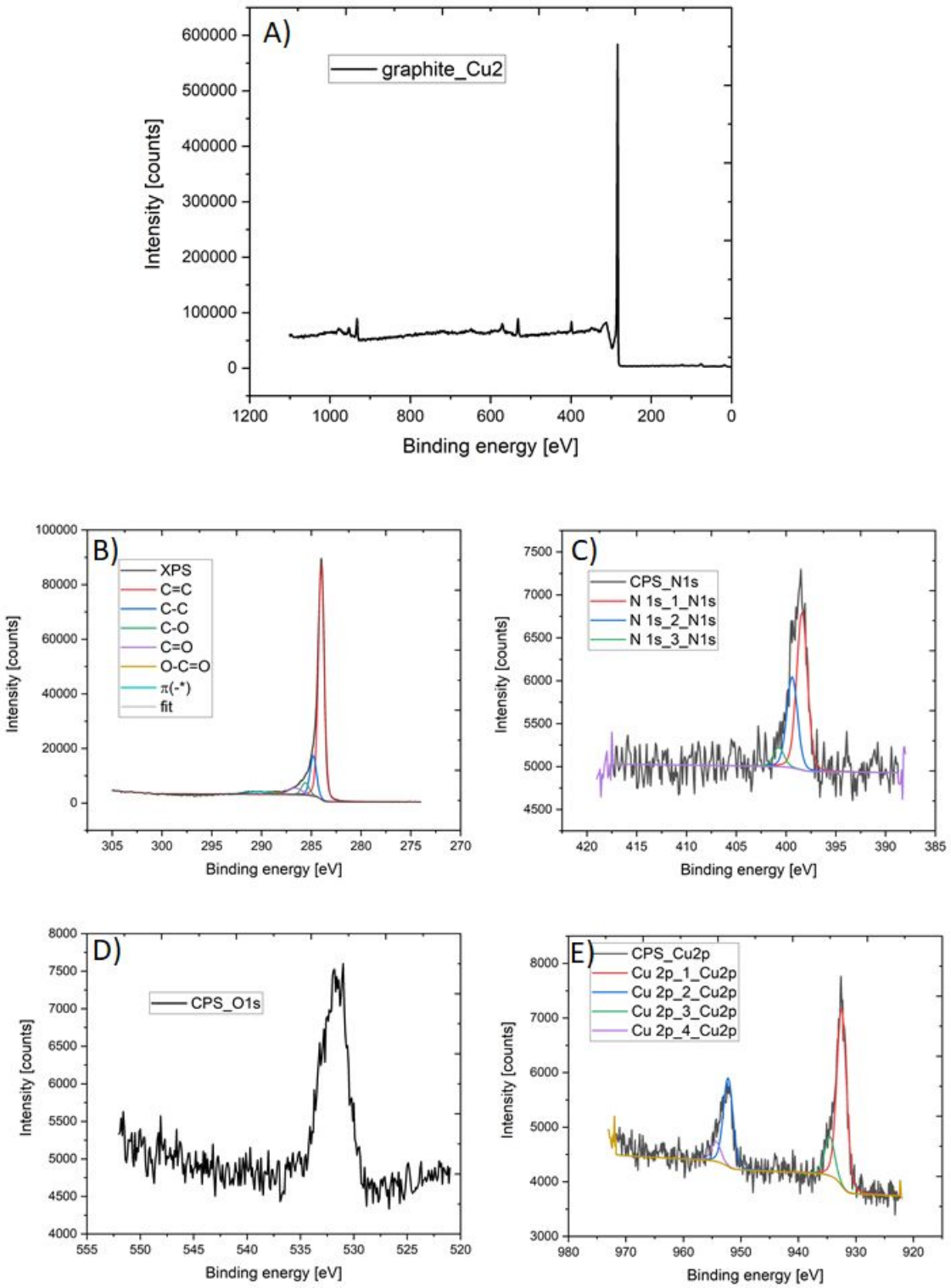

Figure S19: The XPS spectra for graphite-Cu2 sample: A) survey; B) C1s; C) N1s; D) O1s; E) Cu2p core levels.

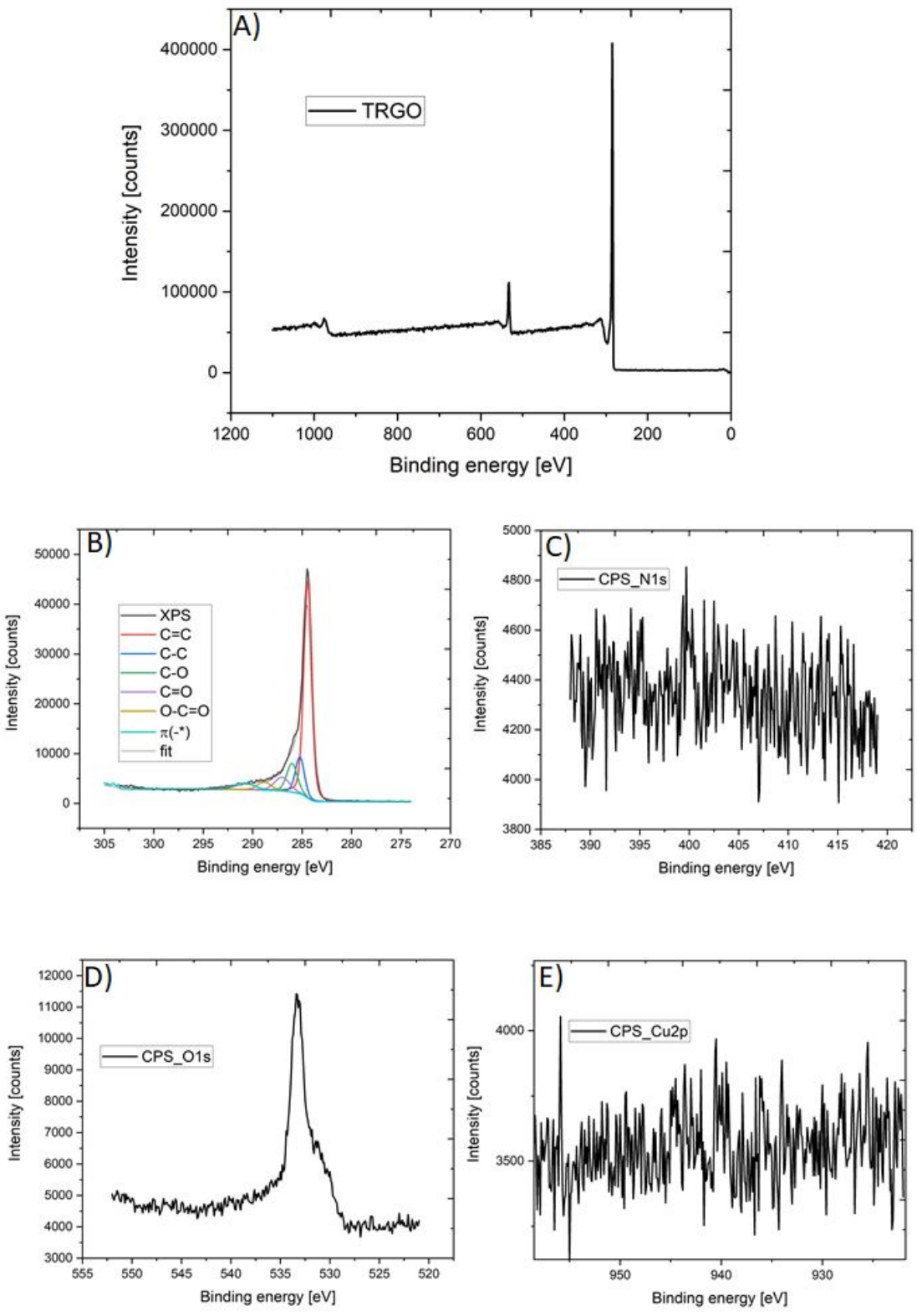

Figure S20: The XPS spectra for TRGO: A) survey; B) C1s; C) N1s; D) O1s; E) Cu2p core levels.

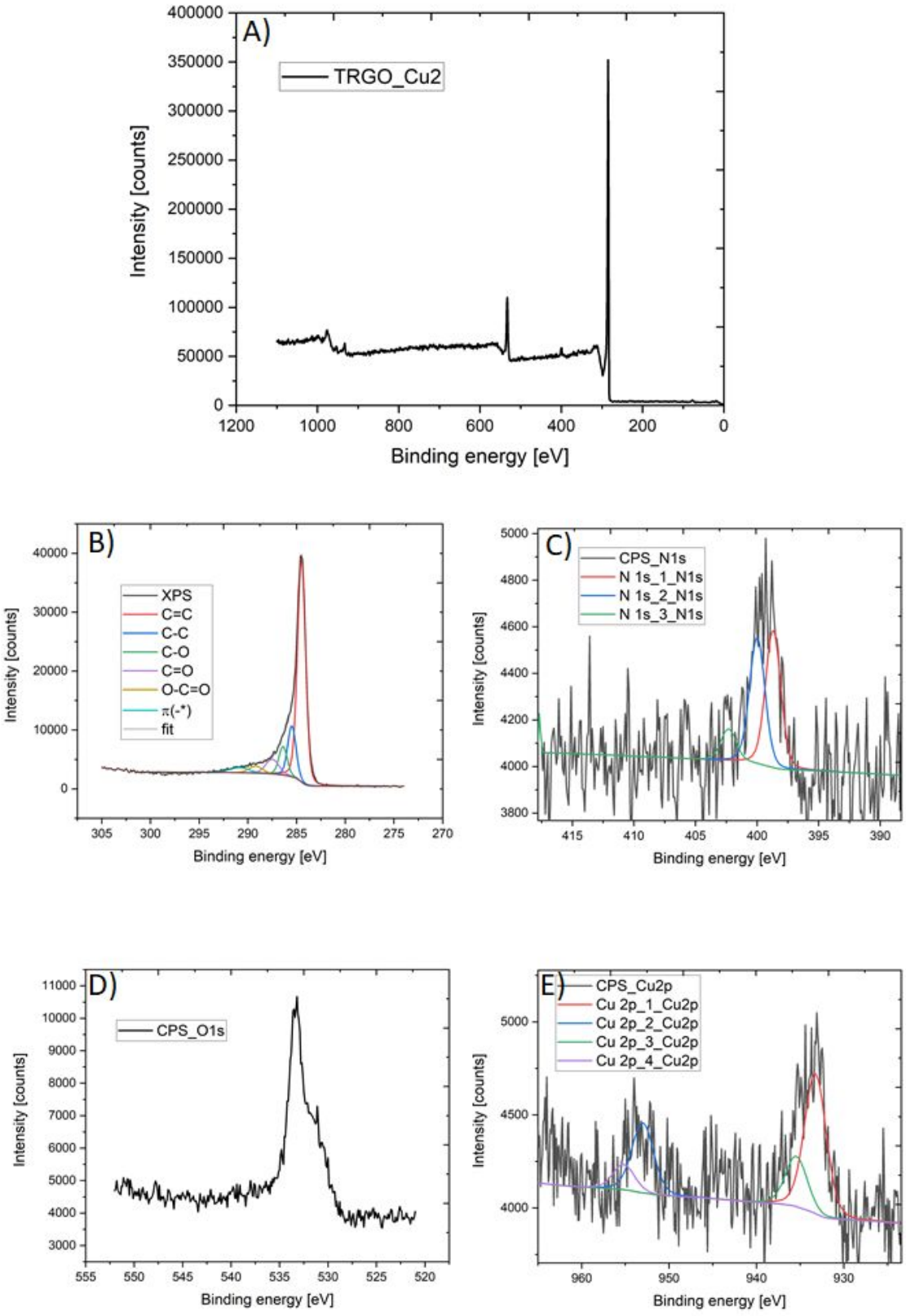

Figure S21: The XPS spectra for TRGO-Cu2: A) survey; B) C1s; C) N1s; D) O1s; E) Cu2p core levels.

Figure S22: The EDX elemental mapping for sample graphite-Cu2.

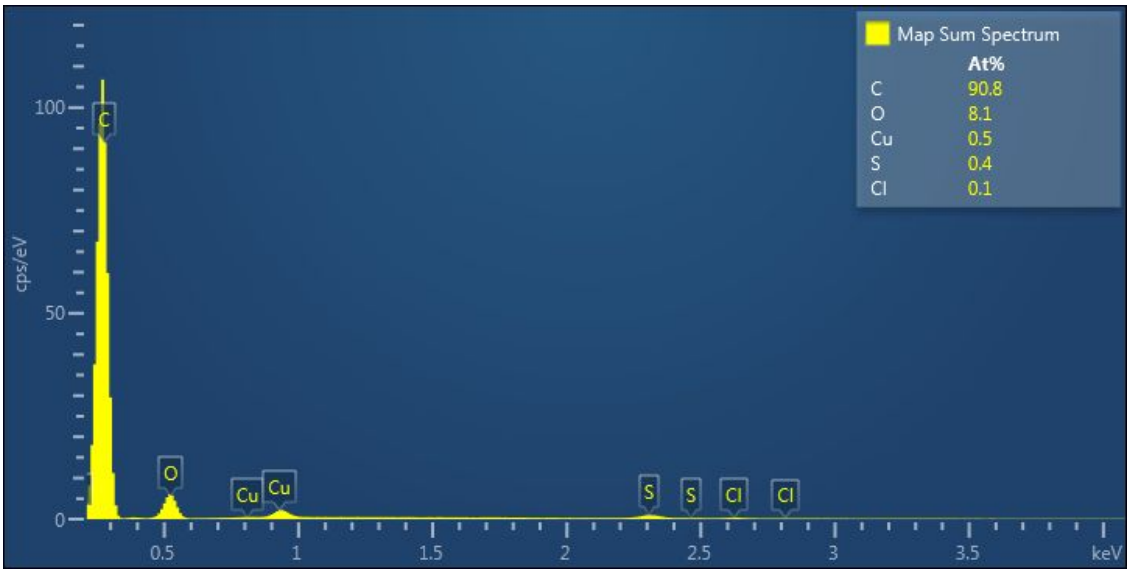

Figure S23: The EDX elemental mapping for sample TRGO-Cu2.

References

[1] Angela Altomare et al. "SIR97: a new tool for crystal structure determination and refinement". In: *Journal of applied crystallography* 32.1 (1999), pp. 115–119.

[2] Ji Chen et al. "An improved Hummers method for eco-friendly synthesis of graphene oxide". In: *Carbon* 64 (2013), pp. 225–229.

[3] Clare F Macrae et al. "Mercury: visualization and analysis of crystal structures". In: *Journal of applied crystallography* 39.3 (2006), pp. 453–457.

[4] Frank Neese and F Wennmohs. "ORCA: an ab initio DFT and semiempirical SCF-MO package". In: *University of Bonn, Bonn, Germany* (2007).

[5] Zbyszek Otwinowski and Wladek Minor. "[20] Processing of X-ray diffraction data collected in oscillation mode". In: *Methods in enzymology*. Vol. 276. Elsevier, 1997, pp. 307–326.

[6] George M Sheldrick and Thomas R Schneider. "[16] SHELXL: High-resolution refinement". In: *Methods in enzymology*. Vol. 277. Elsevier, 1997, pp. 319–343.